Extended Abstracts of the 2005 International Conference on Solid State Devices and Materials, Kobe, 2005, pp.1034-1035

H-8-2

Study of the Metal-Ferroelectric-Insulator-Si Structure Device Formation by Controlling Properties of High Frequency and Microwave Excited Plasma

Ichirou Takahashi, Hiroyuki Sakurai, Tatsunori Isogai[1], Akinobu Teramoto, Shigetoshi Sugawa[1], and Tadahiro Ohmi
Phone: +81-22-795-3977 Fax: +81-22-795-3986 e-mail: ichirou@fff.niche.tohoku.ac.jp
New Industry Creation Hatchery Center, Tohoku University, Sendai 980-8579, Japan
[1]Graduate School of Engineering, Tohoku University, Sendai 980-8579, Japan

1. Introduction

Recently nonvolatile memory devices having ferroelectric gate structure (Metal- Ferroelectric- Insulator- Si Field Effect Transistor (MFIS-FET) structure) have attracted much attention from the viewpoints of high speed, nondestructive readout and high-packing-density memory LSIs. However, there are many problems to be solved, as follows. (a) It is difficult to crystallize ferroelectric on the insulator such as amorphous SiO_2. (b) Because of small coercive field (weak ferroelectricity), the memory window of the MFIS device's CV hysteresys curve tends to be very small. (c) In order to obtain large memory window of it, thick ferroelectric film is needed. (d) As a result, low voltage operation is difficult. We have already reported the ferroelectric formation technology on amorphous insulator and MFIS structure device 3V operation with low dielectric constant ferroelectric $Sr_2(Ta_{1-x},Nb_x)_2O_7$ (STN, x=0.3). These were realized by (1) the thin seed layer formed by rf-sputtering and microwave excited plasma treatment, and (2) the formation of the ferroelectric whose oxygen vacancy is reduced by the Ferroelectric Multi-Layer Stack (FMLS) deposition process [1]. This plasma treatment can oxidize the surface of the film and supply ion bombardment energy to the surface of the film.

In this work, we report the relation between rf-sputtering plasma condition and $Sr_2(Ta_{1-x},Nb_x)_2O_7$ crystal phase on SiO_2 and also reported MFIS structure device's electrical properties. Furthermore, we propose the application of high-density plasma to the ferroelectric improvement.

2. Experimental

Figure 1 shows microwave excited (2.45GHz) high-density ($>10^{12}cm^{-3}$) low electron temperature (<1eV) Kr/O_2 plasma system for improvement of ferroelectric. The detail of rf-sputtering condition of STN is shown in Table I. Figure 4 shows the device structure images and the process flows of MFIS structure device for rf-sputtering plasma dependency experiment. STN is formed on the 10nm STN seed layer/SiO_2(10nm)/Si. The condition of the rf frequency electrode power was changed within the range from 8W to 22W. Based on the results of the experiment, the FMLS-MFIS structure device with STN (100nm, repeating 5nm STN deposition and the plasma treatment 20 times) was fabricated on the adequate plasma condition as shown in Fig. 10.

3. Results and Discussions

Figure 2 shows Leakage current density of Al/as-deposited STN(20nm)/Pt capacitor. Basic rf-sputtering condition is fixed from the viewpoints of the reduction of the leakage current density as shown in Table I. Fig.3 shows our previous results of XRD measurement of the STN on SiO_2 with (sample B) and without (sample A) 10nm STN seed layer [1]. In the case of the sample A, the pattern indicates that $Sr_3(Ta,Nb)_6Si_4O_{26}$ phase grows. On the other hand, in the case of the sample B, (151) peak of the perovskite STN appears and the peaks of $Sr_3(Ta,Nb)_6Si_4O_{26}$ such as (210) are decreasing. This indicates that in order to obtain perovskite STN on SiO_2 it is indispensable to introduce the thin seed layer formed by microwave excited plasma treatment. However, the adequate rf-sputtering plasma condition to form the perovskite STN has not been researched. Figure 5 shows XRD patterns by XRD reciprocal space mapping of 140nm STN on the 10nm STN seed layer/SiO_2/Si and those rf frequency power is 10W(fig. 5(a)), 14W(fig. 5(b)) and 18W(fig. 5(c)). In the case of the fig. 5(a), the XRD patterns are almost similar to those of sample A and this indicates that $Sr_3(Ta,Nb)_6Si_4O_{26}$ phase grows. In the case of the fig. 5(b), (151) peak of perovskite STN appears and the peaks of $Sr_3(Ta,Nb)_6Si_4O_{26}$ such as (210) are decreasing. On the other hand, in the case of the fig. 4(c), the peaks of perovskite STN such as (151) are decreasing. Fig. 6 shows the peak intensity of several crystal phases as a function of rf frequency power. This indicates that perovskite STN has well grown on the condition of 14W rf frequency power. Figure 7 shows the CV hysteresis curves of the IrO_2/STN(140nm)/seed layer(10nm)/SiO_2/Si devices. When rf frequency power is 14W, its memory window is the largest as shown in fig. 7(b). Figure 8 shows the memory window and dielectric constant of the total 150nm STN film as a function of the rf frequency power. The dielectric constant value of the STN that is formed on the condition of 14W rf frequency power is almost equal to those of STN reported previously [2]. These results indicatet that in order to fabricate perovskite STN on amorphous SiO_2 it is important not only to introduce seed layer but also to give the surface of the film adequate Kr^+ ion bombardment energy that corresponds to those of 14W rf power in this case (fig. 9(a)). Another concept to obtain better perovskite STN is (1) to give low ion bombardment energy (below E_a) and (2) irradiate Kr ion to the surface of the film a lot of times to supplement lack of the energy as shown in fig. 9(b). The FMLS-MFIS device formed by high-density low energy ion bombardment plasma shows effectiveness of the concept. Figure 11 (a) and (b) show XRD patterns and CV hysteresis curves of the FMLS-MFIS device, respectively. These results indicate that excellent perovskite STN phase is obtained.

4. Conclusion

We have clarified the relation between ferroelectric crystal phase on amorphous SiO_2 and rf high frequency plasma condition. We have successfully developed a new technology that crystallizes ferroelectric on amorphous insulator by control of the rf high frequency and microwave excited plasma properties.

References

[1] I. Takahashi et al, International Symposium of Integrated Ferroelectric 2005, 1-10-C, P.48 (2005)
[2] Y. Fujimori et al., Jpn. J. Appl. Phys., vol. 38, p. 2285 (1999)

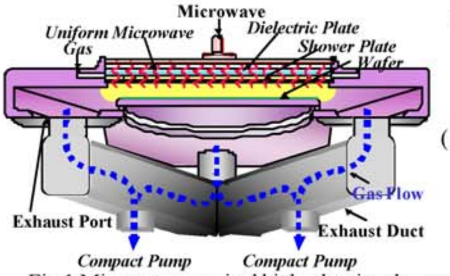

Fig.1 Microwave -excited high -density plasma system.

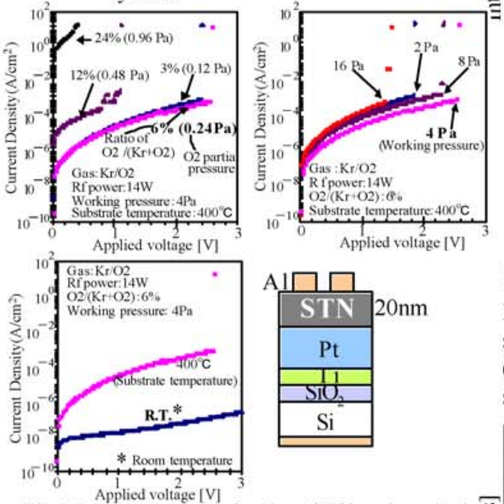

Fig.2 Leakage current density of Al/as-deposited STN(20nm)/Pt capacitor. Figure. (a), (b) and (c) are O_2 partial pressure, working pressure and substrate temperature dependency, respectively.

Table I. Sputtering condition of STN

Experimental parameter \ Film formation	Seed layer (basic Condition)	Deposition for plasma dependency
Rf frequency (MHz)	13.56	13.56
Rf power (W)	14	**8～22**
Gas	Kr/O_2	Kr/O_2
Working pressure (Pa)	4	4
O_2 partial pressure (Pa)	0.24	0.24
Substrate voltage	Floating	Floating
Substrate temperature	R.T.	R.T.

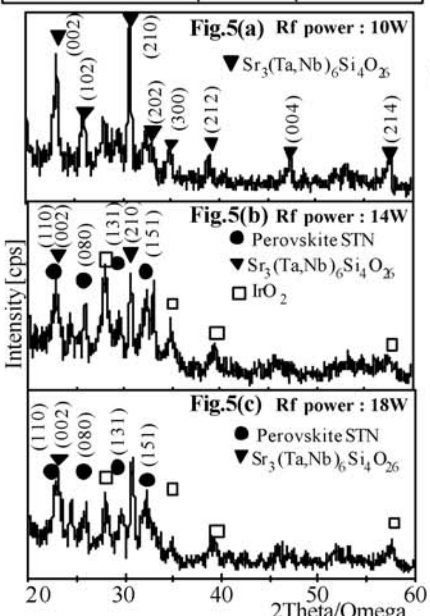

Fig.5 XRD patterns (by XRD reciprocal space mapping) of STN(140nm)/STN seed layer(10nm)/SiO_2 /Si. Rf power of the 13.56 MHz high -frequency electrode during 140nm STN deposition is (a)10W, (b)14W and (c)18W.

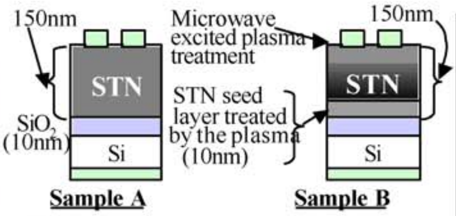

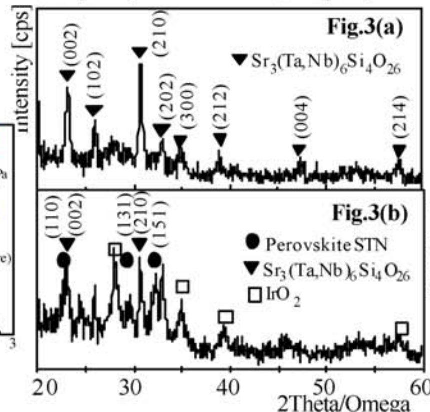

Fig.3 XRD patterns (by XRD reciprocal space mapping) of (a)STN(150nm)/SiO_2 (sample A), (b)STN(140nm)/10nm STN seed layer/SiO_2 (sample B).

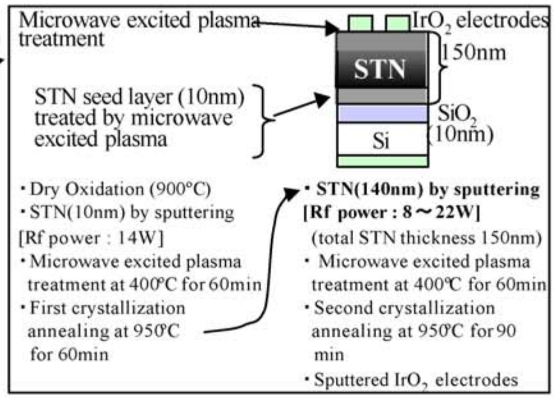

Fig.4 Device structure images and the process flows of MFIS structure devices. This experiment is performed in order to find the most adequate sputtering condition (rf power) for growth of perovskite STN phase.

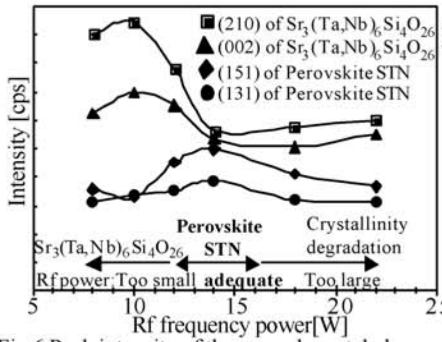

Fig.6 Peak intensity of the several crystal phase on the 10nm seed layer/SiO_2/Si as a function of rf frequency power.

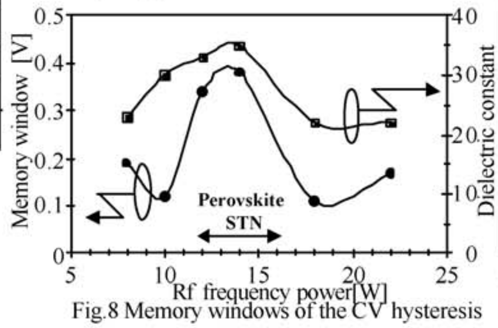

Fig.8 Memory windows of the CV hysteresis curves of the IrO_2/STN(140nm)/STN seed layer(10nm)/SiO_2/Si devices and dielectric constant of the total 150nm STN film as a function of rf frequency power.

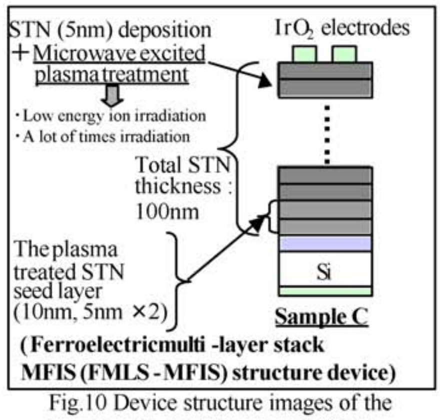

Fig.10 Device structure images of the ferroelectric multi-layer stack MFIS structure device.

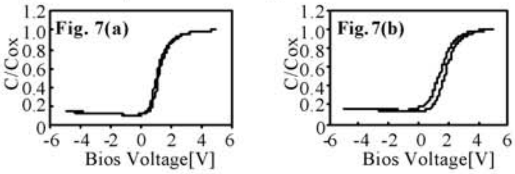

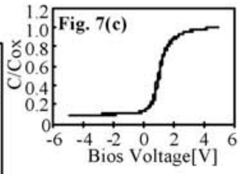

Fig.7 CV curves of the IrO_2/STN(140nm)/STN seed layer (10nm)/SiO_2(10nm) /Si. Rf sputtering power during 140nm STN deposition is 10W (Fig. 7(a)), 14W (fig. 7(b)) and 18W (fig. 7(c)).

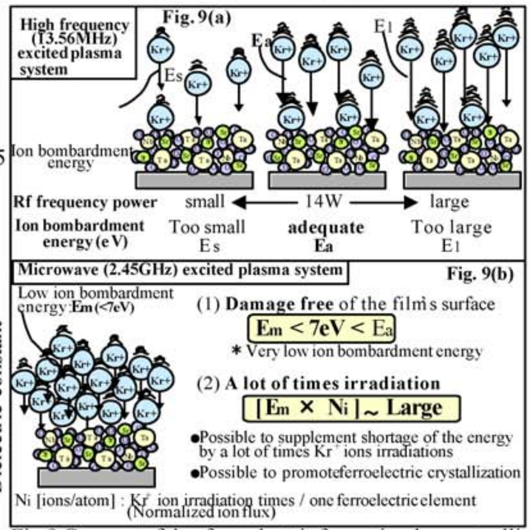

Fig.9 Concept of the ferroelectric formation by controlling the properties of the plasma excited by 13.56MHz high frequency (fig. 9(a)) and microwave (fig. 9(b)).

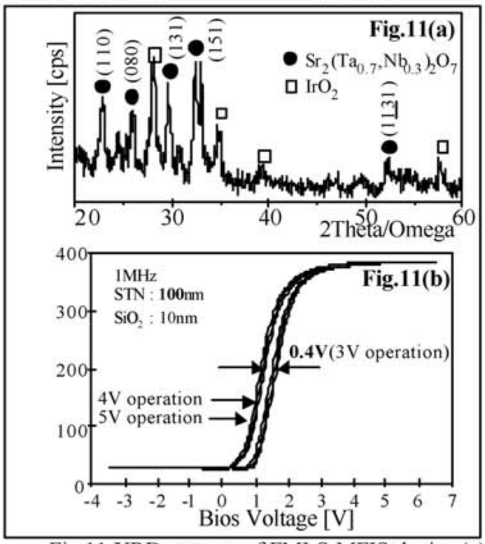

Fig.11 XRD patterns of FMLS-MFIS device (a) and its CV hysteresis curves (b).